Non-magnetic origin of spin Hall magnetoresistance-like signals in Pt films and epitaxial NiO/Pt bilayers

Applied Physics Letters

Non-magnetic origin of spin Hall magnetoresistance-like signals in Pt films and epitaxial NiO/Pt bilayers

Cite as: Appl. Phys. Lett. **116**, 022410 (2020); https://doi.org/10.1063/1.5134814
Submitted: 01 November 2019 . Accepted: 26 December 2019 . Published Online: 14 January 2020

A. Churikova, D. Bono, B. Neltner, A. Wittmann, L. Scipioni, A. Shepard, T. Newhouse-Illige, J. Greer, and G. S. D. Beach

Applied Physics Letters ARTICLE scitation.org/journal/apl

Non-magnetic origin of spin Hall magnetoresistance-like signals in Pt films and epitaxial NiO/Pt bilayers

Cite as: Appl. Phys. Lett. **116**, 022410 (2020); doi: 10.1063/1.5134814
Submitted: 1 November 2019 · Accepted: 26 December 2019 ·
Published Online: 14 January 2020

View Online Export Citation CrossMark

A. Churikova,[1] D. Bono,[1] B. Neltner,[1] A. Wittmann,[1] L. Scipioni,[2] A. Shepard,[2] T. Newhouse-Illige,[2] J. Greer,[2] and G. S. D. Beach[1,a)]

AFFILIATIONS

[1]Department of Materials Science and Engineering, Massachusetts Institute of Technology, Cambridge, Massachusetts 02139, USA
[2]PVD Products, Inc., Wilmington, Massachusetts 01887, USA

[a)]Author to whom correspondence should be addressed: gbeach@mit.edu

ABSTRACT

Electrical control of magnetic order in antiferromagnetic insulators (AFIs) using a Pt overlayer as a spin current source has been recently reported, but detecting and understanding the nature of current-induced switching in AFIs remain a challenge. Here, we examine the origin of spin Hall magnetoresistance-like signals measured in a standard Hall bar geometry, which have recently been taken as evidence of current-induced switching of the antiferromagnetic order in Pt/AFI bilayers. We show that transverse voltage signals consistent with both the partial switching and toggle switching of the Néel vector in epitaxial Pt/NiO bilayers on Al_2O_3 are also present in Pt/Al_2O_3 in which the AFI is absent. We show that these signals have a thermal origin and arise from (i) transient changes in the current distribution due to non-uniform Joule heating and (ii) irreversible changes due to electromigration at elevated current densities, accompanied by long-term creep. These results suggest that more sophisticated techniques that directly probe the magnetic order are required to reliably exclude transport artifacts and thus infer information about the antiferromagnetic order in such systems.

Antiferromagnetic (AF) materials have historically played only a passive role as biasing layers in spintronic applications due to the challenges in manipulating and detecting the magnetic order. However, substituting ferromagnets by antiferromagnets as active switching elements in spintronic devices offers the potential for ultrahigh speed dynamics (terahertz), stability against external magnetic fields, and higher bit packing density due to the lack of stray fields, as well as qualitatively new physical phenomena.[1–5] These advantages have motivated intensive research, most recently in current-induced magnetization switching in both metallic[6–9] and insulating[10–15] AFs.

In metallic AFs (CuMnAs or Mn_2Au), a current-induced staggered spin polarization can rotate the magnetic sublattices and AF spin axis via the Néel spin–orbit torque (NSOT).[16–21] In antiferromagnetic insulators (AFIs), the Néel order can be switched by the antidamping spin–orbit torque (SOT) generated by the spin accumulation from the spin Hall effect (SHE)[22] in an adjacent heavy metal (HM) layer without the need for an external field.[23] Switching by antidamping SOT does not require that the spin sublattices form inversion partners as in NSOT switching,[16] and hence, it is a more general approach that may enable all-electrical control over a wider variety of AFs. In AF/heavy-metal (HM) heterostructures, the spin Hall magnetoresistance (SMR)[24] can be used for the electrical detection of sublattice switching and Néel vector orientation,[25–27] where longitudinal (R_{xx}) and transverse (R_{xy}) resistances vary by the relative angle between the Néel vector in the AF and the orientation of the spin polarization created by the SHE in an adjacent HM layer.[24]

Recently published studies of AFI/HM bilayers provided the first steps toward the electrical control and detection of the Néel order.[10–13] Two types of transverse Hall signal signatures after current pulse injection have been attributed to AF phenomena, but their origins are contended. Reference 10 reported a saw-tooth-shaped change R_{xy} while injecting a series of switching current pulses in epitaxial, biaxially strained NiO(001). The results were interpreted as arising from partial SOT switching of a multidomain state, where the Néel order rotated in the direction of the writing current along one of the easy axes.[10] In epitaxial Pt/NiO(111)/Pt trilayers in Ref. 11, the Néel order was believed

to rotate orthogonal to the writing current due to additive SOTs from the Pt layers. The steplike R_{xy} shape was attributed to toggle-switching between two distinct magnetic states[11] and in Ref. 12 to the spin-transport across the NiO(001)/Pt interface.[12] Very recent works found evidence for nonmagnetic contributions to R_{xy} in the Pt layer used for SOT switching and suggested that the saw-tooth-like signal is a parasitic effect, whereas the steplike signal is of magnetic origin.[12,14,15]

In this Letter, we show that all transport features previously identified as SMR from an AFI are also present in isolated Pt layers on a nonmagnetic substrate and can be attributed to two mechanisms: read current path deviations in the device following localized Joule heating and Pt electromigration (EM) following large current pulses that ultimately causes irreversible device degradation. We show that simple interpretations of transport measurements cannot be reliably used to infer information about the magnetic state of AFIs.

Epitaxial NiO films of thicknesses 5, 25, and 50 nm were grown on $Al_2O_3(0001)$ substrates at 600 °C by off-axis radio frequency magnetron sputtering[28,29] from a NiO target (off-axis angle, 45°) at 5 mTorr (2.5 sccm of O_2, 47.5 sccm Ar). The epitaxial growth and strain state of NiO films were confirmed with a high-resolution x-ray diffraction 2θ-ω coupled scan of the (111) reflection and reciprocal space maps (see the supplementary material). On top of NiO and bare Al_2O_3 substrates, we grew Pt(5 nm) by magnetron sputtering. The continuous layers were patterned into four-arm Hall cross devices with 10×40 μm arm dimensions using optical photolithography.

Figure 1(a) shows the Hall cross geometry and current configurations used to attempt current-induced switching of the Néel vector by 90° and SMR detection. Write current pulses I_w with 1 ms width were injected such that the current in the center flowed approximately along +45° (Write 1) and −45° (Write 2) relative to the read current

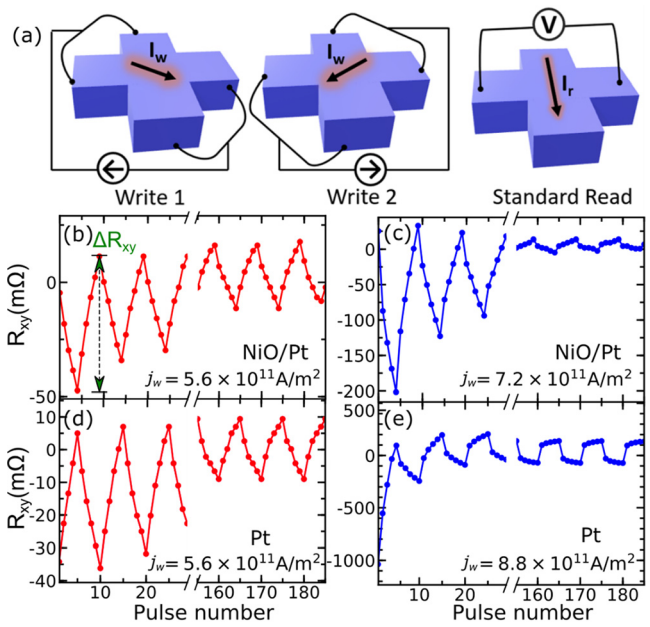

FIG. 1. (a) Schematic of current orientations used in the experiment. The switching signal from (b) and (c) NiO(50 nm)/Pt(5 nm) and (d) and (e) Pt(5 nm) is shown for increasing j_w.

direction. The read current I_r probes the transverse Hall resistance R_{xy}. In the case where R_{xy} is purely of SMR origin, $R_{xy} = \Delta R_{xy}^{SMR} \sin 2\varphi$, where φ is the angle between the Néel vector and the current direction and ΔR_{xy}^{SMR} is the SMR coefficient.[24] Complete SOT switching of the AF order should orient the Néel vector at ±45° current pulse configurations, which should switch R_{xy} between $\pm\Delta R_{xy}^{SMR}$. However, in our work and others,[12,14,15] the SMR signal in NiO/Pt is masked by parasitic contributions to R_{xy}.

To show this, we injected write current pulse sequences with a fixed amplitude and recorded R_{xy} 10 s after each write pulse (to minimize transient thermal effects[10]) with a small read current (I_r = 1 mA and current density $j_r = 2 \times 10^{10}$ A/m^2). Figures 1(b) and 1(c) show a periodic change in R_{xy} in NiO(50 nm)/Pt(5 nm) bilayers while applying current pulse sequences of five Write 1 followed by five Write 2 pulses (see the full current range in the supplementary material). A saw-tooth R_{xy} signal is observed for the first five cycles for both low ($j_w = 5.6 \times 10^{11}$ A/m^2) in Fig. 1(b) and high ($j_w = 7.2 \times 10^{11}$ A/m^2) current densities in Fig. 1(c) but relaxes to a more steplike shape at high j_w, as seen after 16 cycles following the axis break. We define the peak-to-peak magnitude of R_{xy} for a single cycle of Write 1-Write 2 pulses as ΔR_{xy}, illustrated in Fig. 1(b). When NiO was omitted, a persistent saw-tooth signal was also observed for low j_w in Pt in Fig. 1(d). At high j_w, continuous device cycling reveals a relaxation to a steplike signal, which persists after 18 cycles [Fig. 1(e)]. We show that both types of R_{xy} signal shapes can originate from the bare Pt layer and cannot be used to confirm the R_{xy} origin.

In both NiO/Pt and Pt, ΔR_{xy} declines in magnitude considerably after a series of cycles at high j_w, suggesting irreversible device damage at these densities. At $j_w = 7.2 \times 10^{11}$ A/m^2, we observe an irreversible decline in the maximum ΔR_{xy}, which is thought to originate from device breakdown or irreversible switching occurring at the highly heated corners of the device.[20] When current pulses of lower amplitude were again applied to the same device, ΔR_{xy} did not return to its original magnitude. Thus, it is necessary to study the mechanisms that lead to device breakdown, as they may affect the detected resistance before any visible damage occurs.

To examine the behavior of R_{xy} caused by Joule heating from current pulses, we plot the maximum ΔR_{xy} reached for each j_w as a function of increasing j_w in Pt and NiO/Pt bilayers with NiO thicknesses of 5, 25, and 50 nm in Fig. 2(a) (see the source in the supplementary material). While the behavior is exponential for lower current values, ΔR_{xy} saturates at higher current densities. Although no NiO thickness dependence of threshold j_w has previously been reported,[10–12] we found that the current threshold is significantly smaller for Pt devices on NiO(50 nm). As the thermal conductivity of NiO is smaller than that of Al_2O_3, the rate of heat dissipation is lower in the NiO(50 nm)/Pt bilayer. This suggests that the mechanism behind the R_{xy} signal from the Pt layer is thermally driven. Meanwhile, the Joule heating for this range of j_w is estimated to contribute to a temperature rise ΔT between 70 K (at the first detectable signal measured) and 260 K (at the point of irreversible degradation) during the duration of the pulse (see the supplementary material).

To confirm the role of heating, we recorded R_{xy} during a sequence of write pulses with $j_w = 5.6 \times 10^{11}$ A/m^2 at temperatures T = 25, 45, and 65 °C, while the samples were in good thermal contact with the heating stage. Figures 2(b) and 2(c) show the T-dependent R_{xy} in fresh NiO(50 nm)/Pt(5 nm) and Pt(5 nm) films, respectively,

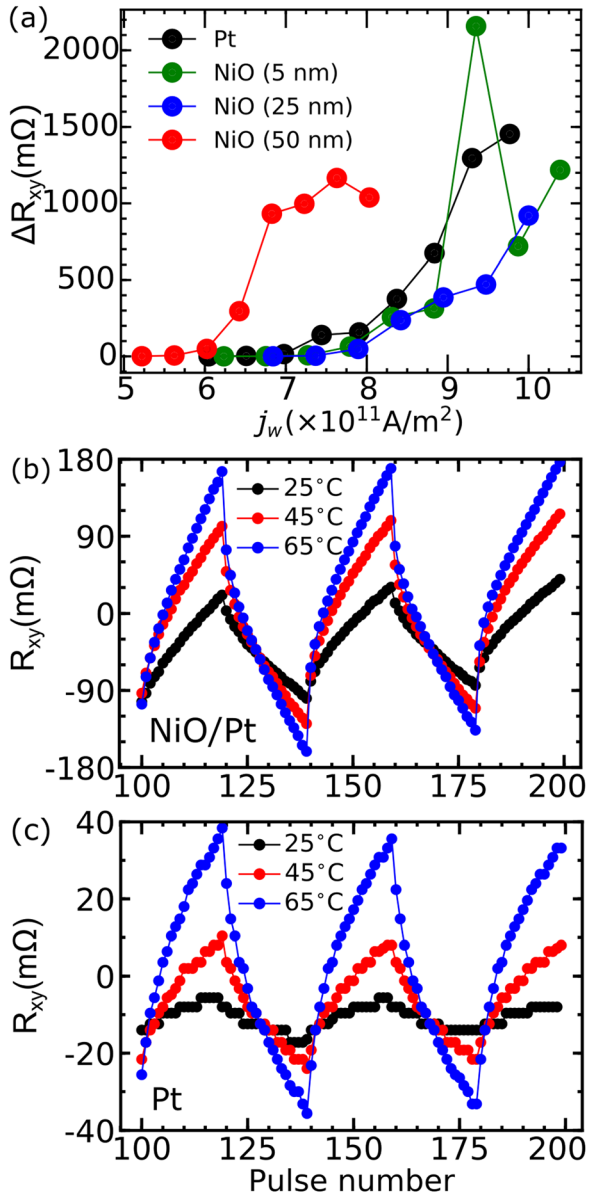

FIG. 2. (a) Current density (j_w) dependence of maximal change in switching amplitude ΔR_{xy} for the Pt film and for NiO/Pt (5 nm) layers of varying NiO thicknesses. (b) Temperature-dependent R_{xy} for NiO(50 nm)/Pt(5 nm) and (c) Pt(5 nm).

after 100 pulses when the signal equilibrated. ΔR_{xy} increases with increasing substrate T in both materials, mirroring the increase in ΔR_{xy} as a function of j_w. A thermally generated and/or activated mechanism is thus likely responsible for the signal change in both cases.

To consider the symmetry of the parasitic R_{xy} in Pt, we averaged four "read" measurements of read configurations each rotated by 90°, after each write pulse [Fig. 3(a)]. This approach has been previously used to eliminate parasitic R_{xx} contributions due to geometric effects in a similar device.[30] In Fig. 3(a), a single read current configuration produces a saw-tooth signal, while an average of four read

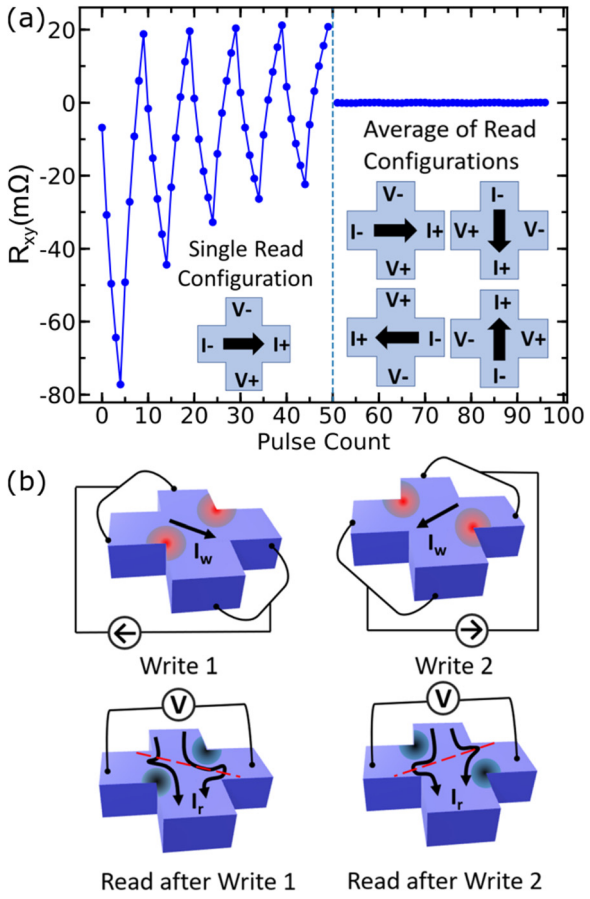

FIG. 3. (a) R_{xy} as a function of pulse count when (left) a single read current configuration and (right) an average of four read configurations are used. (b) The schematic shows the possible thermal origin of the R_{xy} signal following I_w application.

configurations eliminates the signal entirely, eliminating the possibility of any out-of-plane contribution to the R_{xy} signal.

We propose a mechanism that contributes to an in-plane symmetry breaking in Pt. When I_w is applied to the Hall cross, j_w and thus the Joule heating are the highest around the two constricting corners [red spots in Fig. 3(b)]. Consequently, the resistivity of these "hot spots" increases, leading to a significant asymmetry in the I_r paths. This generates a R_{xx} contribution to R_{xy}, which depends on the previous I_w, resulting in a positive (negative) resistance for Write 1 (Write 2), and the "saw-tooth" shape. Thus, increasing T (via substrate heating or Joule heating) increases the resistance of the devices and the contribution from the thermoresistive effect to ΔR_{xy}. When these localized hot spots reach certain T thresholds, the device becomes irreversibly damaged.

Finally, to directly confirm these irreversible changes to the Pt layer after current pulse injection, we used scanning electron microscopy (SEM) to image corners of four different devices. Figure 4(a) shows a fresh device. The device in Fig. 4(b) has undergone 6 write cycles with a saw-tooth R_{xy} signal ($I_w = 6.7 \times 10^{11}$ A/m^2) and shows formation of small hillocks. In Fig. 4(c), void formation is observed in a device that has been pulsed with 6 write cycles with larger current

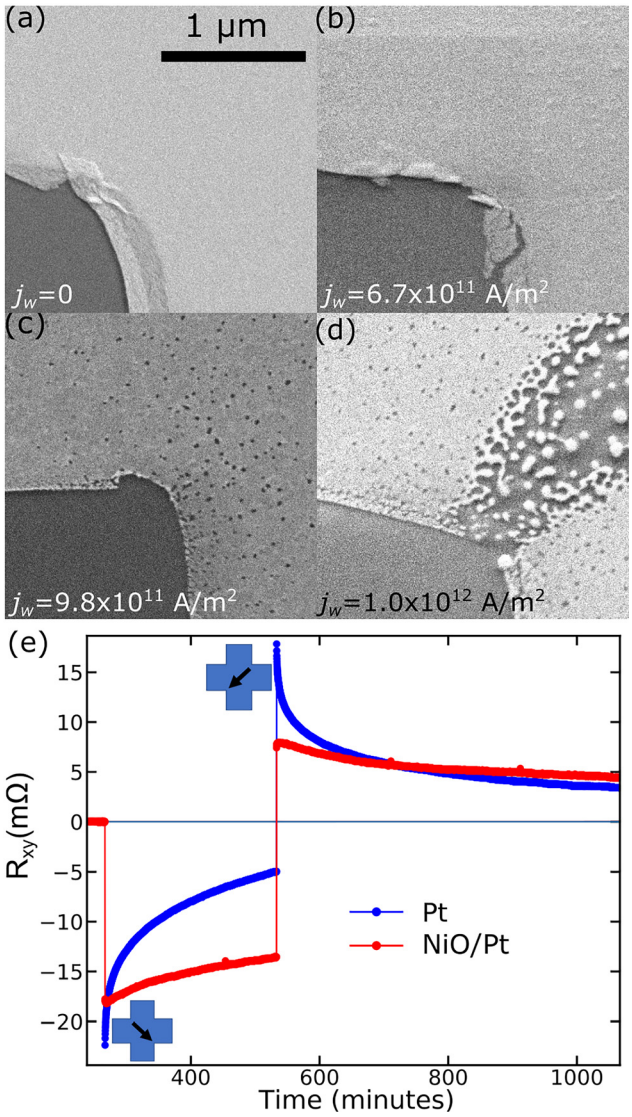

FIG. 4. (a)–(e) SEM micrographs of corners of four different Pt(5 nm) Hall cross devices after the application of 6 cycles of varying j_w to each, where the light (dark) gray areas are the Pt device (substrate). (b) Long-time relaxation of the R_{xy} signal after Write 1 and Write 2 pulses in (blue) Pt(5 nm) on the sapphire substrate and (red) Pt(5 nm) on NiO(50 nm).

densities ($I_w = 9.8 \times 10^{11}$ A/m^2), with R_{xy} having equilibrated to a steplike signal. In Fig. 4(d), hemispherical electrically separated islands are observed after device breakdown ($I_w = 1.0 \times 10^{12}$ A/m^2). This is a characteristic manifestation of electromigration that eventually leads to migration-induced breakdown beginning at the corners. The Pt grain boundaries acting as sources and sinks for point defects may be responsible for the long-term relaxation of R_{xy} following a write pulse, as EM diffusional creep has produced similar relaxation behavior for current densities on the order of 10^{10} A/m^2 in Al and Cu thin film interconnects.[31] This diffusional creep may be reflected in the long-term R_{xy} relaxation following a write pulse. In Fig. 4(b), R_{xy} is recorded continuously first after a single Write 1 pulse and then a single Write 2 pulse for both Pt and NiO/Pt. In Pt, R_{xy} does not equilibrate back to the initial state after many hours, which indicates a permanent change in the system, likely due to EM-induced structural deformation (see the supplementary material for details).

In summary, we demonstrate experimentally that the switching-like signal observed in Pt is due to in-plane symmetry breaking and originates in localized thermoresistive heating. The signal can take the form of both a saw-tooth and a steplike shape, which has been previously attributed to AF switching. We bring attention to the irreversible device damage following typical current densities used in SMR experiments, which could make any detected SMR switching irreproducible. Finally, to extract the SMR contribution to the transverse resistance, one needs to mitigate Joule heating effects at constrictions (creating the saw-tooth signal) and the transient and long-term impacts of electromigration (immediately changing the local device resistance and gradual relaxation due to point defect diffusion following read measurements). We suggest that systematic studies of activation energies for thermal migration may additionally yield understanding of the long-term structural changes to the Pt layer, which manifest in the transverse resistance signal. Our results imply that more sophisticated methods that do not rely solely on the electrical signal from the metal overlayer[9,14,32] are required to detect the AF order. Furthermore, our findings open venues for further studies on the role of the heavy-metal overlayer structural integrity and quality on such parasitic heating effects and emphasize the general importance of more careful consideration of all possible contributions to a thermally induced signal (e.g., choice of substrate and current pulse characteristics).

See the supplementary material for complete structural characterization and current-dependent switching measurements.

This work was supported by SMART, a center of nCORE, a Semiconductor Research Corporation program, sponsored by the National Institute of Standards and Technology (NIST). This work made use of the Shared Experimental Facilities supported in part by the MRSEC Program of the National Science Foundation under Award No. DMR-1419807. A.C. thanks Felix Büttner, Can Onur Avci, Kai Litzius, and Ethan Rosenberg for fruitful discussion and Charles Settens and James Daley for technical support.

REFERENCES

[1]T. Kampfrath, A. Sell, G. Klatt, A. Pashkin, S. Mährlein, T. Dekorsy, M. Wolf, M. Fiebig, A. Leitenstorfer, and R. Huber, Nat. Photonics **5**, 31 (2011).
[2]T. Jungwirth, X. Marti, P. Wadley, and J. Wunderlich, Nat. Nanotechnol. **11**, 231 (2016).
[3]T. Shiino, S.-H. Oh, P. M. Haney, S.-W. Lee, G. Go, B.-G. Park, and K.-J. Lee, Phys. Rev. Lett. **117**, 087203 (2016).
[4]K. Garello, C. O. Avci, I. M. Miron, M. Baumgartner, A. Ghosh, S. Auffret, O. Boulle, G. Gaudin, and P. Gambardella, Appl. Phys. Lett. **105**, 212402 (2014).
[5]V. Lopez-Dominguez, H. Almasi, and P. K. Amiri, Phys. Rev. Appl. **11**, 024019 (2019).
[6]P. Wadley, B. Howells, J. Železný, C. Andrews, V. Hills, R. P. Campion, V. Novak, K. Olejnik, F. Maccherozzi, S. S. Dhesi, S. Y. Martin, T. Wagner, J. Wunderlich, F. Freimuth, Y. Mokrousov, J. Kune, J. S. Chauhan, M. J. Grzybowski, A. W. Rushforth, K. W. Edmonds, B. L. Gallagher, and T. Jungwirth, Science **351**, 587 (2016).
[7]S. Yu. Bodnar, L. Šmejkal, I. Turek, T. Jungwirth, O. Gomonay, J. Sinova, A. A. Sapozhnik, H.-J. Elmers, M. Kläui, and M. Jourdan, Nat. Commun. **9**, 348 (2018).

[8]K. Olejník, V. Schuler, X. Marti, V. Novák, Z. Kašpar, P. Wadley, R. P. Campion, K. W. Edmonds, B. L. Gallagher, J. Garces, M. Baumgartner, P. Gambardella, and T. Jungwirth, Nat. Commun. **8**, 15434 (2017).
[9]M. J. Grzybowski, P. Wadley, K. W. Edmonds, R. Beardsley, V. Hills, R. P. Campion, B. L. Gallagher, J. S. Chauhan, V. Novak, T. Jungwirth, F. Maccherozzi, and S. S. Dhesi, Phys. Rev. Lett. **118**, 057701 (2017).
[10]X. Z. Chen, R. Zarzuela, J. Zhang, C. Song, X. F. Zhou, G. Y. Shi, F. Li, H. A. Zhou, W. J. Jiang, F. Pan, and Y. Tserkovnyak, Phys. Rev. Lett. **120**, 207204 (2018).
[11]T. Moriyama, K. Oda, T. Ohkochi, M. Kimata, and T. Ono, Sci. Rep. **8**, 14167 (2018).
[12]L. Baldrati, A. Ross, T. Niizeki, C. Schneider, R. Ramos, J. Cramer, O. Gomonay, M. Filianina, T. Savchenko, D. Heinze, A. Kleibert, E. Saitoh, J. Sinova, and M. Kläui, Phys. Rev. B **98**, 024422 (2018).
[13]I. Gray, T. Moriyama, N. Sivadas, G. M. Stiehl, J. T. Heron, R. Need, B. J. Kirby, D. H. Low, K. C. Nowack, D. G. Schlom, D. C. Ralph, T. Ono, and G. D. Fuchs, Phys. Rev. X **9**, 041016 (2019).
[14]Y. Cheng, S. Yu, M. Zhu, J. Hwang, and F. Yang, e-print arXiv:1906.04694 [Cond-Mat].
[15]P. Zhang, J. Finley, T. Safi, and L. Liu, Phys. Rev. Lett. **123**, 247206 (2019).
[16]J. Železný, H. Gao, K. Výborný, J. Zemen, J. Mašek, A. Manchon, J. Wunderlich, J. Sinova, and T. Jungwirth, Phys. Rev. Lett. **113**, 157201 (2014).
[17]O. Gomonay, T. Jungwirth, and J. Sinova, Phys. Rev. Lett. **117**, 017202 (2016).
[18]J. Železný, H. Gao, A. Manchon, F. Freimuth, Y. Mokrousov, J. Zemen, J. Mašek, J. Sinova, and T. Jungwirth, Phys. Rev. B **95**, 014403 (2017).
[19]X. F. Zhou, J. Zhang, F. Li, X. Z. Chen, G. Y. Shi, Y. Z. Tan, Y. D. Gu, M. S. Saleem, H. Q. Wu, F. Pan, and C. Song, Phys. Rev. Appl. **9**, 054028 (2018).
[20]M. Meinert, D. Graulich, and T. Matalla-Wagner, Phys. Rev. Appl. **9**, 064040 (2018).
[21]J. Železný, P. Wadley, K. Olejník, A. Hoffmann, and H. Ohno, Nat. Phys **14**, 220 (2018).
[22]A. Hoffmann, IEEE Trans. Magn. **49**, 5172 (2013).
[23]H. V. Gomonay and V. M. Loktev, Phys. Rev. B **81**, 144427 (2010).
[24]Y.-T. Chen, S. Takahashi, H. Nakayama, M. Althammer, S. T. B. Goennenwein, E. Saitoh, and G. E. W. Bauer, Phys. Rev. B **87**, 144411 (2013).
[25]K. Ganzhorn, J. Barker, R. Schlitz, B. A. Piot, K. Ollefs, F. Guillou, F. Wilhelm, A. Rogalev, M. Opel, M. Althammer, S. Geprägs, H. Huebl, R. Gross, G. E. W. Bauer, and S. T. B. Goennenwein, Phys. Rev. B **94**, 094401 (2016).
[26]G. R. Hoogeboom, A. Aqeel, T. Kuschel, T. T. M. Palstra, and B. J. van Wees, Appl. Phys. Lett. **111**, 052409 (2017).
[27]J. Fischer, O. Gomonay, R. Schlitz, K. Ganzhorn, N. Vlietstra, M. Althammer, H. Huebl, M. Opel, R. Gross, S. T. B. Goennenwein, and S. Geprägs, Phys. Rev. B **97**, 014417 (2018).
[28]B. Peters, A. Alfonsov, C. G. F. Blum, S. J. Hageman, P. M. Woodward, S. Wurmehl, B. Büchner, and F. Y. Yang, Appl. Phys. Lett. **103**, 162404 (2013).
[29]F. Yang and P. Chris Hammel, J. Phys. D: Appl. Phys. **51**, 253001 (2018).
[30]T. Kosub, M. Kopte, R. Hühne, P. Appel, B. Shields, P. Maletinsky, R. Hübner, M. O. Liedke, J. Fassbender, O. G. Schmidt, and D. Makarov, Nat. Commun. **8**, 13985 (2017).
[31]E. Glickman, N. Osipov, A. Ivanov, and M. Nathan, J. Appl. Phys. **83**, 100 (1998).
[32]P. Wadley, S. Reimers, M. J. Grzybowski, C. Andrews, M. Wang, J. S. Chauhan, B. L. Gallagher, R. P. Campion, K. W. Edmonds, S. S. Dhesi, F. Maccherozzi, V. Novak, J. Wunderlich, and T. Jungwirth, Nat. Nanotechnol. **13**, 362 (2018).